

Design and Optical Investigations of a Spironaphthoxazine/Spiropyran/Polyoxometalate Triad

Ali Saad, Olivier Oms, Anne Dolbecq, Jérôme Marrot, Khadija Hakouk, Houda El Bekkachi,
Stéphane Jobic, Philippe Deniard, Rémi Dessapt, Damien Garrot, Kamel Boukheddaden, Rongji
Liu, Guangjin Zhang, Bineta Keita and Pierre Mialane

Supporting Information available: X-ray crystallographic files, in CIF format for **MnMo₆O₁₈(SP)(SN)** and **MnMo₆O₁₈(SN)₂** (the TBA cations could not be located properly in the structure due to severe disorder and the data set was corrected with the program SQUEEZE,ⁱ a part of the PLATON package of crystallographic software used to calculate the solvent or counter-ion disorder area and to remove its contribution to the overall intensity data), the ¹H NMR spectra of **MnMo₆O₁₈(SP)(SN)**, **MnMo₆O₁₈(SN)₂** (Figure SI1) and **(SP)₃MnMo₆O₁₈(SN)₂** (Figure SI3), the ¹³C NMR spectra of **MnMo₆O₁₈(SP)(SN)**, **MnMo₆O₁₈(SN)₂** (Figure SI2) and **(SP)₃MnMo₆O₁₈(SN)₂** (Figure SI4), a table containing the crystallographic data for **MnMo₆O₁₈(SP)(SN)** (Table SI1) and **MnMo₆O₁₈(SN)₂** (Table SI2), the oxidation cyclic voltammograms of **MnMo₆O₁₈(SN)₂** (Figure SI5) and **MnMo₆O₁₈(SP)(SN)** (Figure SI6), the reduction cyclic voltammograms of **MnMo₆O₁₈(SN)₂**, **MnMo₆O₁₈(SP)(SN)** (Figure SI7) and **SNTris** (Figure SI8), the UV-near-vis absorption spectra of **SNTris**, **MnMo₆O₁₈(SN)₂** and **MnMo₆O₁₈(SP)(SN)** (Figure SI9), a table containing their characteristics of UV-Visible absorption spectra (Table SI3), pictures related to the electrolysis of **MnMo₆O₁₈(SP)(SN)** (Figure SI10) and **SNTris** (Figure SI11), the Kubelka-Munk transformed reflectivity of all the compounds, $(TBA)_3[MnMo_6O_{18}\{(OCH_2)_3CNH_2, SP_7Na[(Mo_3O_8)_4(O_3PC(C_3H_6NH_3)(O)PO_3)_4]\cdot30H_2O$ and **SPTris** (Figures SI12a, SI12b and SI13), the temporal evolution of the photo-generated absorption of **SNTris** (Figure SI14), **(SP)₃MnMo₆O₁₈(SN)₂** and **(SP)I** (Figure SI15), the $Abs^{584}(t)$ vs. t plots for **(SP)₃MnMo₆O₁₈(SN)₂** and **(SP)I** (Figure SI16), a table containing the photoloration kinetics parameters of all the compounds at room temperature (Table SI4) as well as two tables containing the fading kinetics parameters (under yellow light irradiation and in the dark) of all the compounds at room temperature (Tables SI5 and SI6), the cyclability of **MnMo₆O₁₈(SN)₂** (Figure SI17), the temporal evolutions of the absorption during fading processes for **(SP)₃MnMo₆O₁₈(SN)₂** (Figure SI18) and its cyclability (Figure SI19), the evolutions of the absorption vs. luminous exposure for **MnMo₆O₁₈(SN)₂** (Figure SI20) and **MnMo₆O₁₈(SP)₂** (Figure SI21), the temporal evolutions of the reflectance signal for **MnMo₆O₁₈(SN)₂** at different temperatures (Figure SI22) and two tables containing the photo-coloration kinetic parameters of **MnMo₆O₁₈(SP)₂** (Table SI7) and **MnMo₆O₁₈(SN)₂** (Table SI8) for different temperatures.

Figure SI1. Top: Compared ^1H NMR (CD_3CN) spectra of $\text{MnMo}_6\text{O}_{18}(\text{SP})_2$, $\text{MnMo}_6\text{O}_{18}(\text{SN})_2$ and $\text{MnMo}_6\text{O}_{18}(\text{SP})(\text{SN})$; bottom: zoom on ^1H NMR (CD_3CN) spectrum of $\text{MnMo}_6\text{O}_{18}(\text{SP})(\text{SN})$.

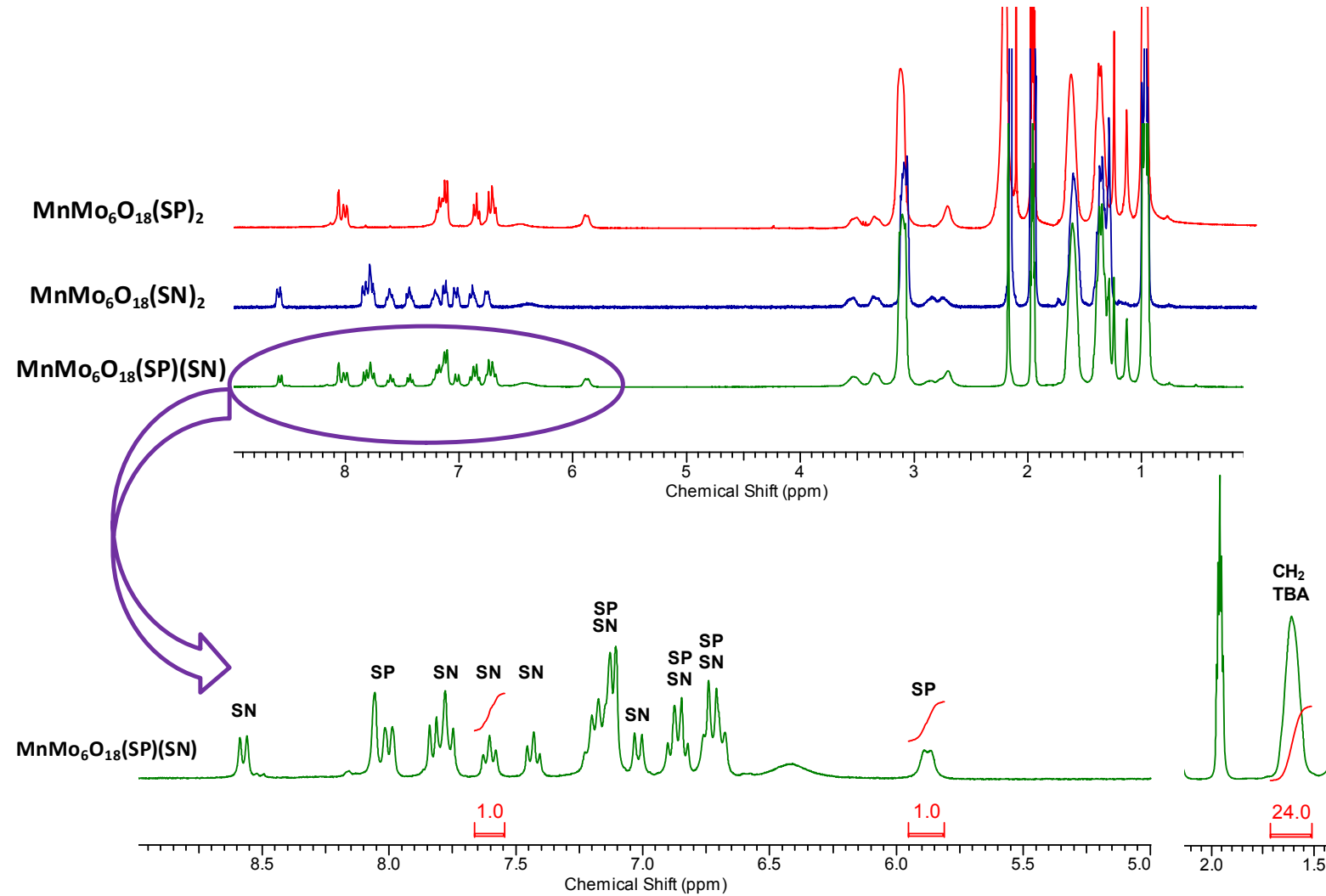


Figure SI2. Compared ^{13}C NMR (CD_3CN) spectra of $\text{MnMo}_6\text{O}_{18}(\text{SN})_2$ and $\text{MnMo}_6\text{O}_{18}(\text{SP})(\text{SN})$.

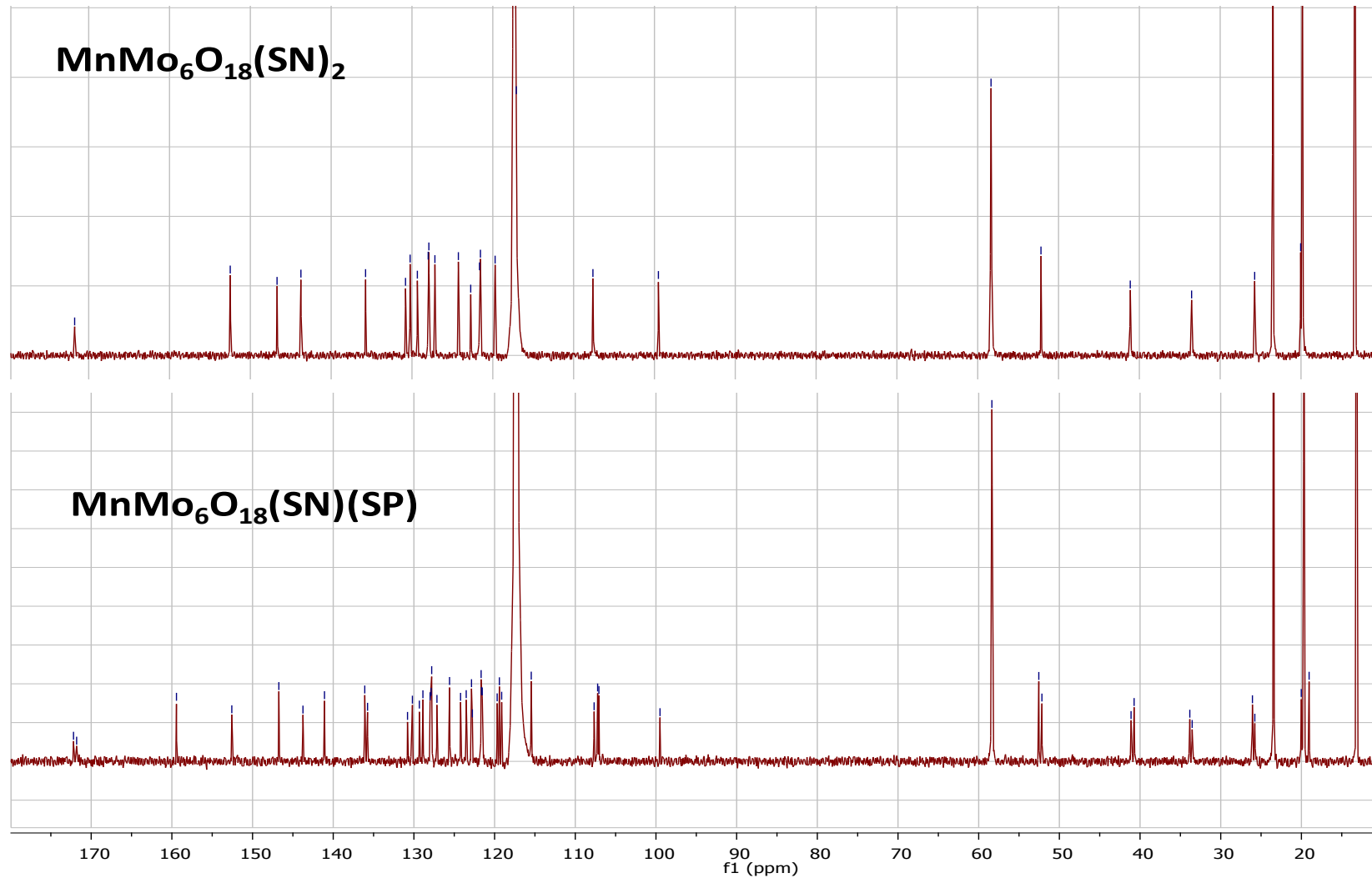


Figure SI3. ^1H NMR (CD_3CN) spectra of $(\text{SP})_3\text{MnMo}_6\text{O}_{18}(\text{SN})_2$.

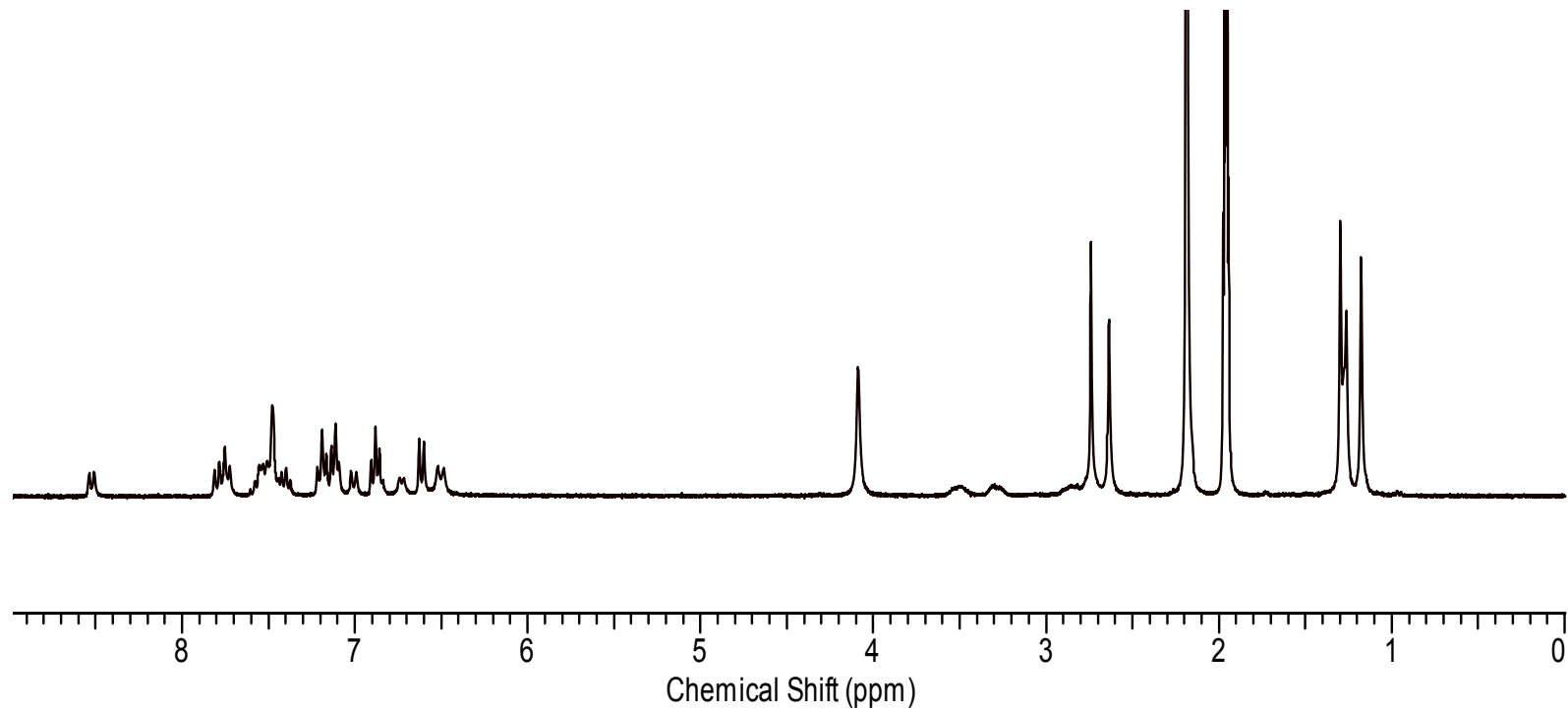


Figure SI4. ^{13}C NMR (CD_3CN) spectra of $(\text{SP})_3\text{MnMo}_6\text{O}_{18}(\text{SN})_2$.

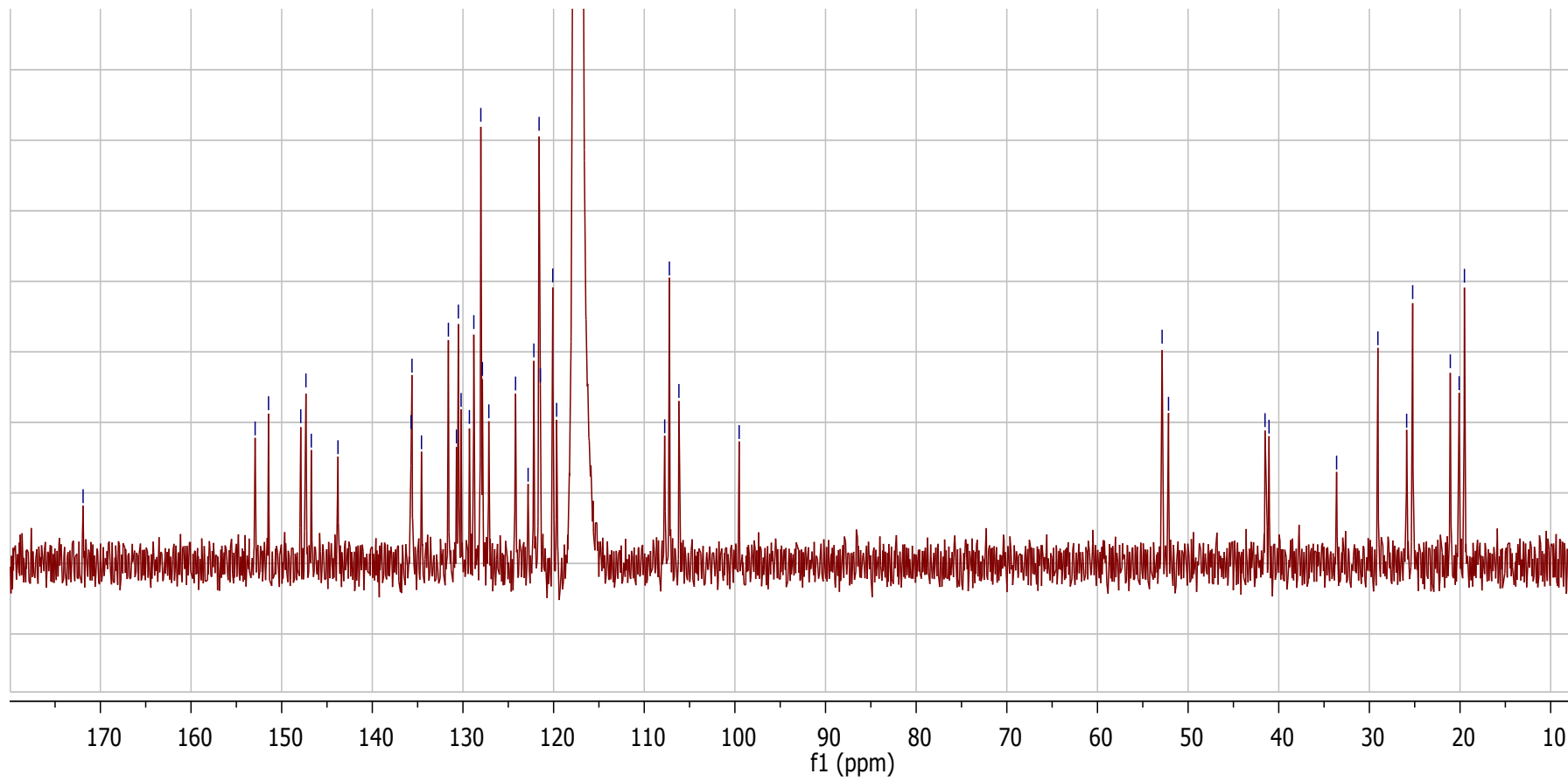


Figure SI5. Oxidation cyclic voltammogram of 0.3 mM $\text{MnMo}_6\text{O}_{18}(\text{SN})_2$ (Mn center). The electrolyte was DMF + 0.2M LiClO₄. The reference electrode was a saturated calomel electrode (SCE). The scan rate was 0.1V s⁻¹.

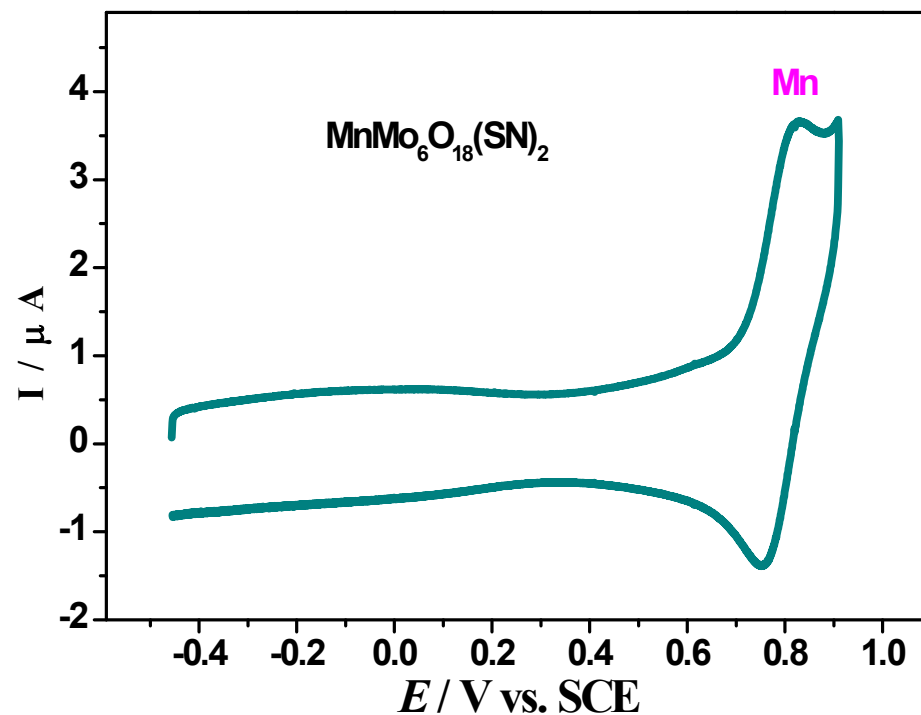


Figure SI6. Oxidation cyclic voltammograms of 0.3 mM **MnMo₆O₁₈(SP)(SN)** (Mn, SP and SN centers). The electrolyte was DMF + 0.2M LiClO₄. The reference electrode was a saturated calomel electrode (SCE). The scan rate was 0.1V s⁻¹.

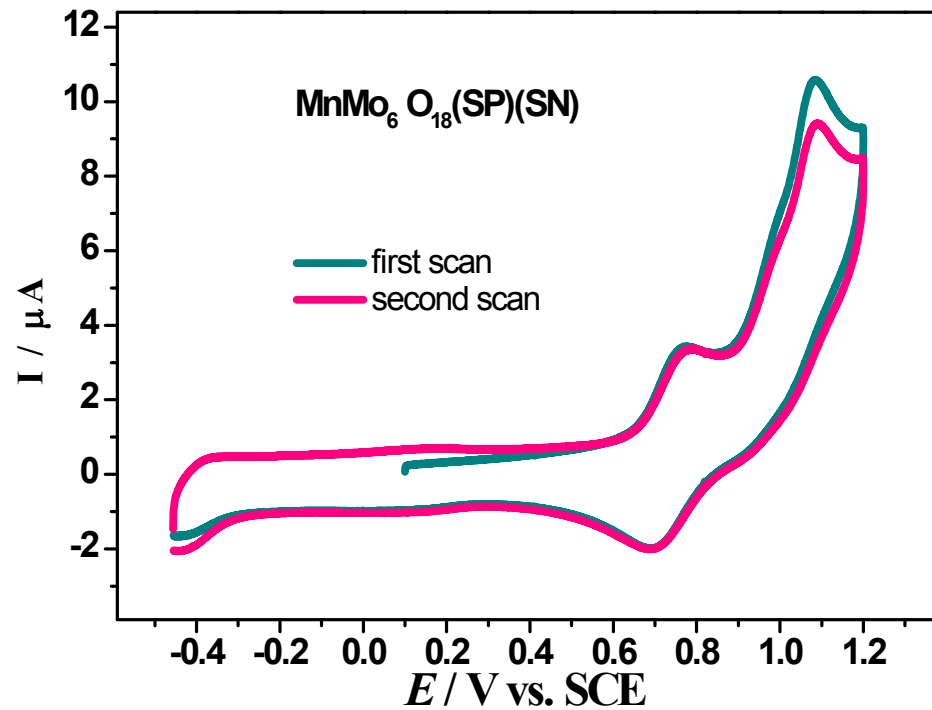


Figure SI7. Reduction cyclic voltammograms. (A) 0.3 mM $\text{MnMo}_6\text{O}_{18}(\text{SN})_2$ (Mn, SN and Mo centers); (B) 0.3 mM $\text{MnMo}_6\text{O}_{18}(\text{SP})(\text{SN})$ (Mn, SP, SN and Mo centers). The electrolyte was DMF + 0.2M LiClO₄. The reference electrode was a saturated calomel electrode (SCE). The scan rate was 0.1 V s⁻¹.

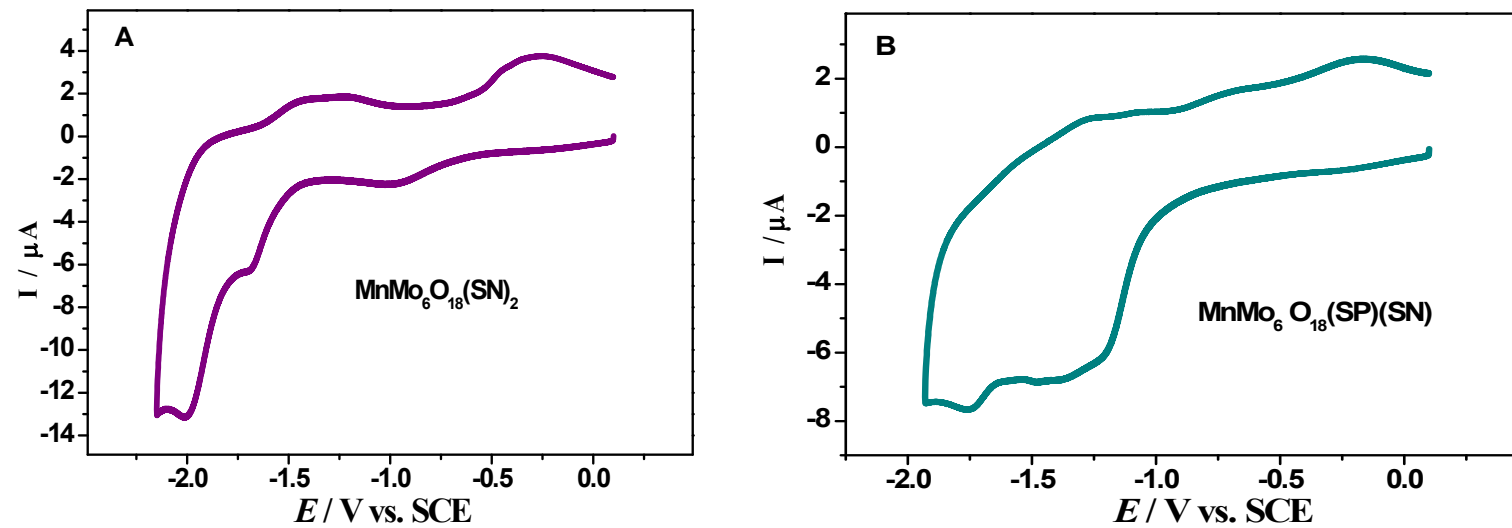


Figure SI8. Reduction cyclic voltammogram of 0.3 mM SNTris (SN center). The electrolyte was DMF + 0.2M LiClO₄.The reference electrode was a saturated calomel electrode (SCE). The scan rate was 0.1V.s⁻¹.

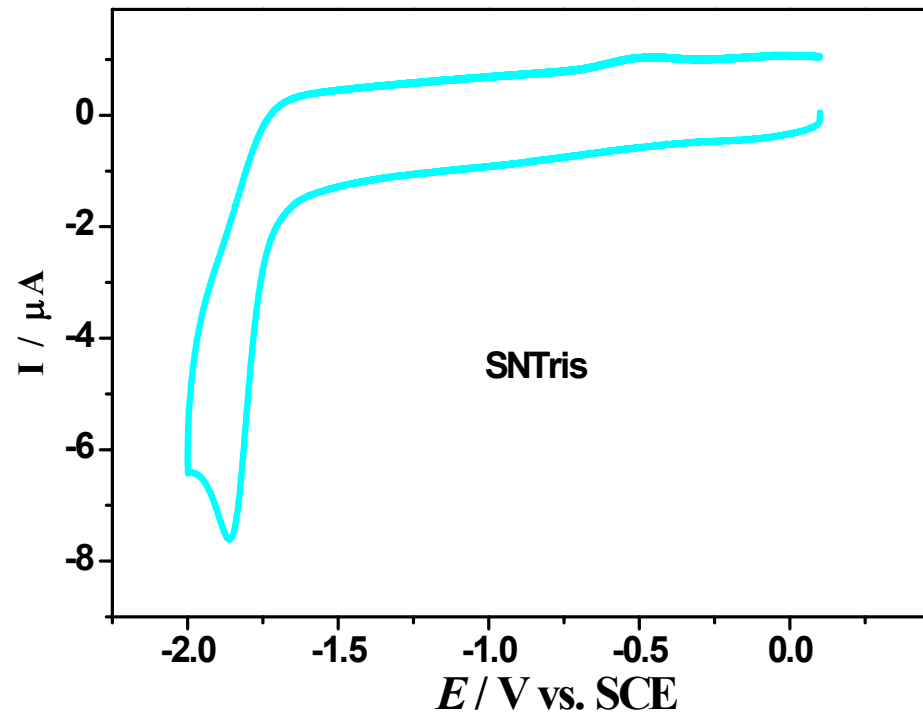


Figure SI9. UV-visible absorption spectra of **SNTris**, **MnMo₆O₁₈(SN)₂** and **MnMo₆O₁₈(SP)(SN)** in DMF + 0.2M LiClO₄.

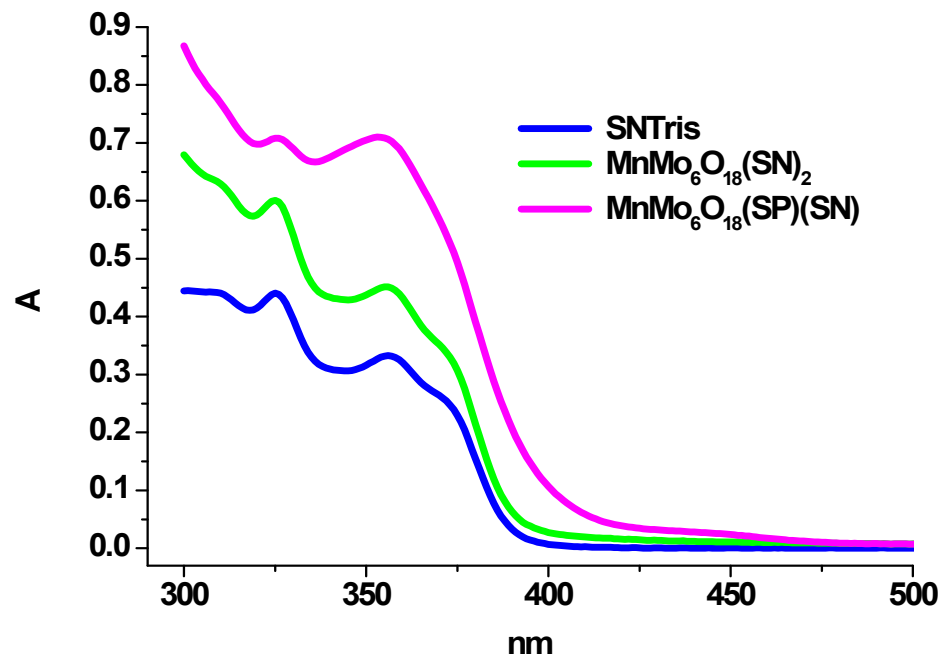


Figure SI10. Observed color nuances: (1) before electrolysis; (2 - 5) coloration during electro-oxidation of 0.15 mM $\text{MnMo}_6\text{O}_{18}(\text{SP})(\text{SN})$; (6- 8) electrochemical fading process by reduction.

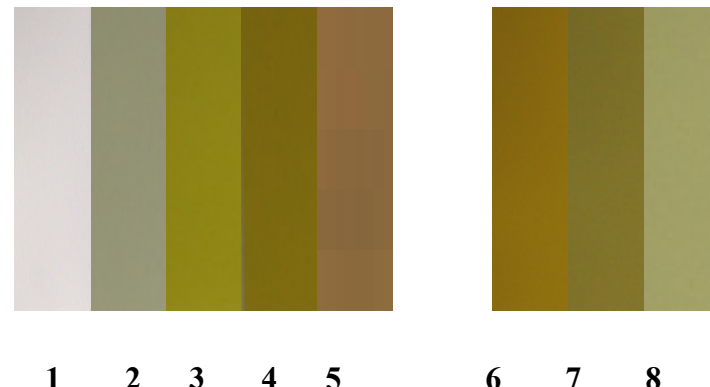


Figure SI11. Observed color nuances: (1) before electrolysis; (2 - 5) coloration during electro-oxidation of 0.6 mM SNTris .



Figure SI12. Kubelka-Munk transformed reflectivity vs wavelength and energy of (a) $\text{MnMo}_6\text{O}_{18}(\text{SN})_2$ (red), $\text{SNT}\text{r}\text{i}\text{s}$ (blue), and $(\text{TBA})_3[\text{MnMo}_6\text{O}_{18}\{\text{(OCH}_2)_3\text{CNH}_2\}_2]$ (black), (b) $(\text{SP})_3\text{MnMo}_6\text{O}_{18}(\text{SN})_2$ (red), $\text{MnMo}_6\text{O}_{18}(\text{SN})_2$ (blue) and $\text{SP}_7\text{Na}[(\text{Mo}_3\text{O}_8)_4(\text{O}_3\text{PC}(\text{C}_3\text{H}_6\text{NH}_3)(\text{O})\text{PO}_3)_4]\cdot 30\text{H}_2\text{O}^{9\text{b}}$ (magenta).

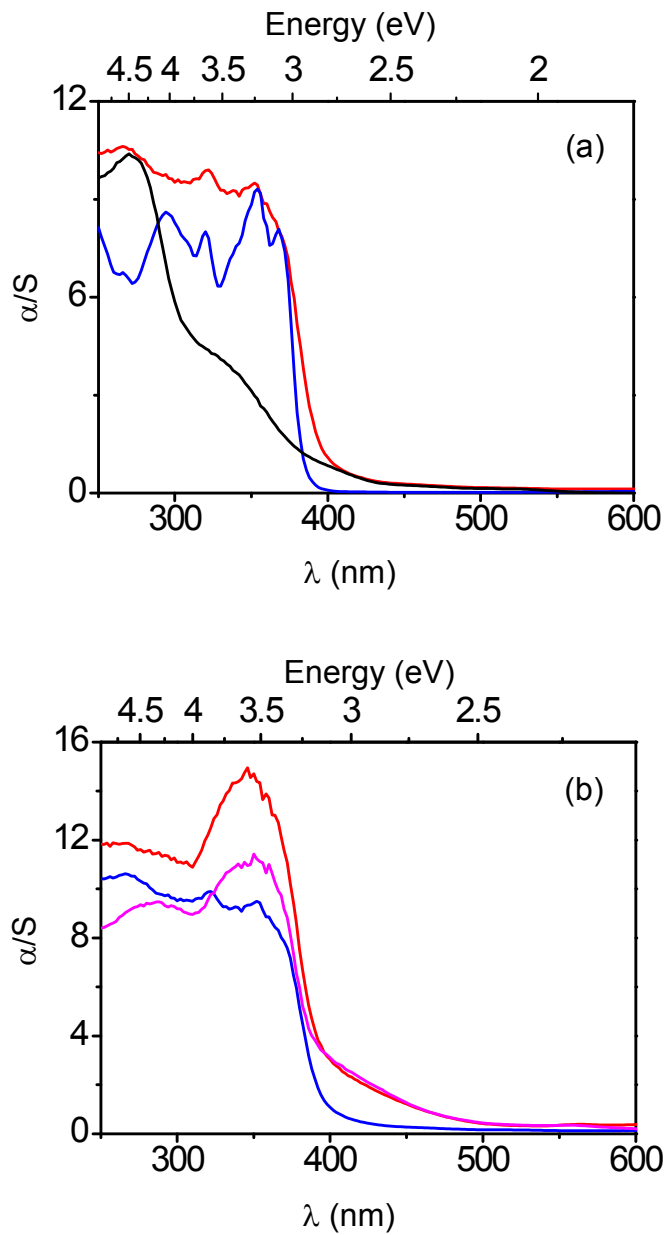


Figure SI13. Kubelka-Munk transformed reflectivity vs wavelength and energy of **MnMo₆O₁₈(SP)(SN)** (—), **SNTris** (—), **SPTris^{10a}** (—) and (TBA)₃[MnMo₆O₁₈{(OCH₂)₃CNH₂}₂] (—). The weak absorptions in the visible in the spectra of **MnMo₆O₁₈(SP)(SN)**, and **SPTris** are assignable to a small amount of the opened “merocyanine” form which is responsible for the color of the powdered samples.

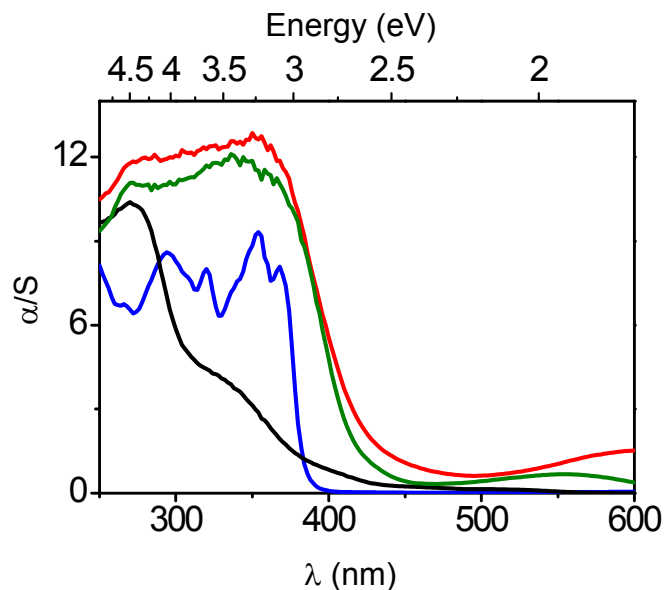


Figure SI14. Temporal evolution of the photo-generated absorption Abs(*t*) of **SNTris** after 0, 0.5, 1, 1.5, 2, 3, 5, 10, 15, 20, and 60 min of 365 nm-UV irradiation.

NB: the color change of the pure organic **SNTris** is quasi undetectable by human eyes, even after irradiating the sample for a period as long as few hours.

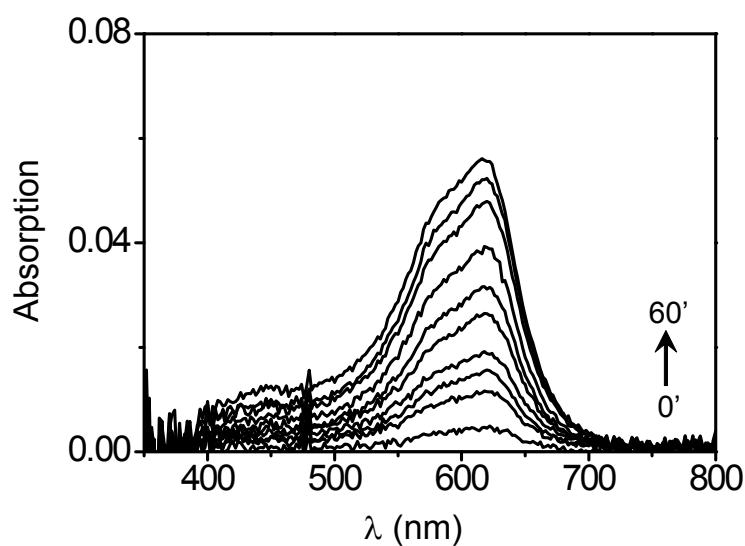


Figure SI15. Temporal evolution of the photogenerated absorption of $(\text{SP})_3\text{MnMo}_6\text{O}_{18}(\text{SN})_2$ and $(\text{SP})\text{I}$ after 0, 0.166, 0.5, 1, 1.5, 2, 3, 4, 6, and 8 min of 365 nm-UV irradiation.

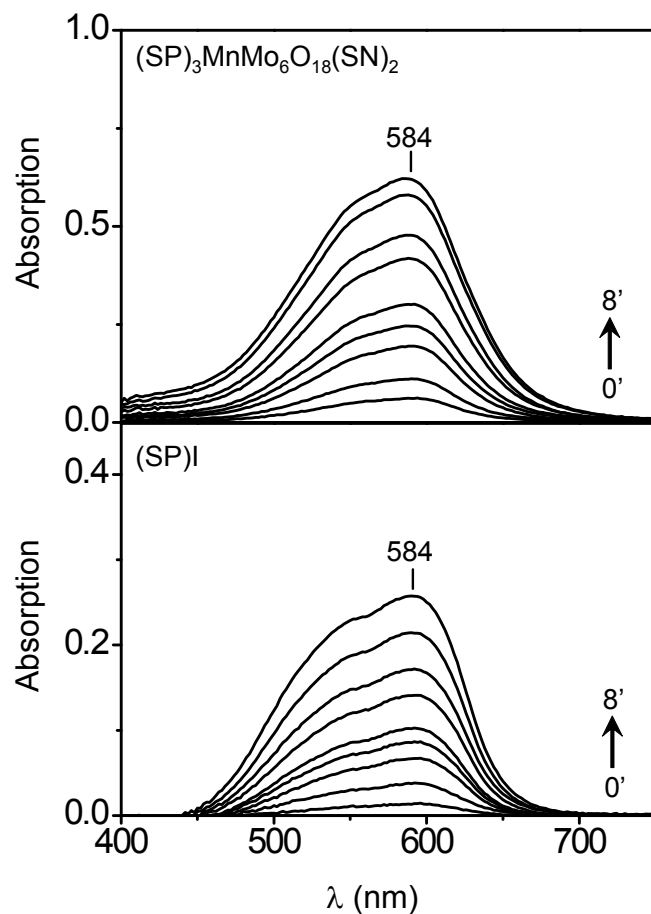


Figure SI16. $\text{Abs}^{584}(t)$ vs. t plots for $(\text{SP})_3\text{MnMo}_6\text{O}_{18}(\text{SN})_2$, and $(\text{SP})\text{I}$. The lines show the fits of the plots according to rate law $\text{Abs}^{584}(t) = -(A_1 + A_2) + A_1 \exp(-k^{c_1}t) + A_2 \exp(-k^{c_2}t)$.

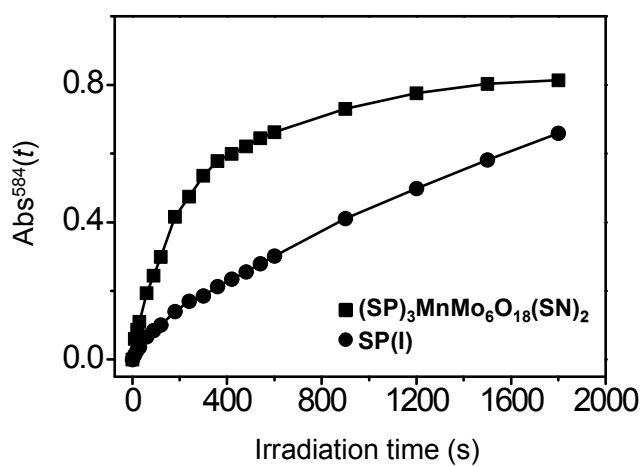


Figure SI17. Evolution of the maximum of the photogenerated absorption at $\lambda_{\max} = 620$ nm for $\text{MnMo}_6\text{O}_{18}(\text{SN})_2$ during successive coloration/bleach cycles at room temperature. For one cycle, the sample is exposed to 365-nm UV irradiation for 1 min, and to yellow light for 30 min (the black lines display the mean values of the absorption in the coloured and bleached states).

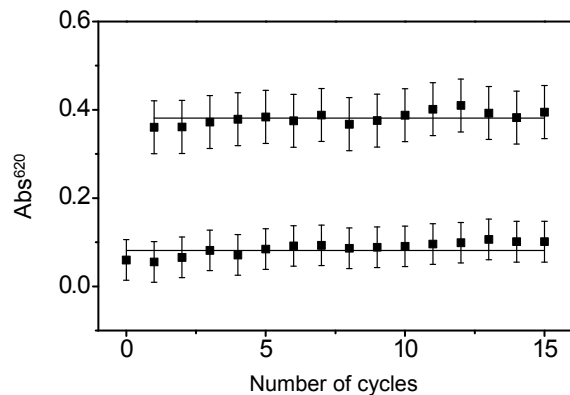


Figure SI18. Temporal evolutions at room temperature of the absorbance at $\lambda_{\max} = 584$ nm for $(\text{SP})_3\text{MnMo}_6\text{O}_{18}(\text{SN})_2$, under 365 nm-UV irradiation (■), in the dark during the thermal fading of a sample initially irradiated for 15 min under 365 nm-UV excitation (○), and under yellow light for a sample initially irradiated for 15 min under 365 nm-UV excitation (△). The lines show the fits of the $\text{Abs}^{584}(t)$ vs t plots according to rate laws $\text{Abs}^{584}(t) = -(A_1 + A_2) + A_1 \exp(-k^c_1 t) + A_2 \exp(-k^c_2 t)$ for the photo-coloration process, and $\text{Abs}^{584}(t) = (A_0 - A_1 - A_2) + A_1 \exp(-k^f_1 t) + A_2 \exp(-k^f_2 t)$ for the two fading ones. The dashed line shows the absorbance value just before switching off the UV irradiation. The percents of absorbance lost after 360 min in the dark (in blue) and under yellow light (in pink) are also indicated.

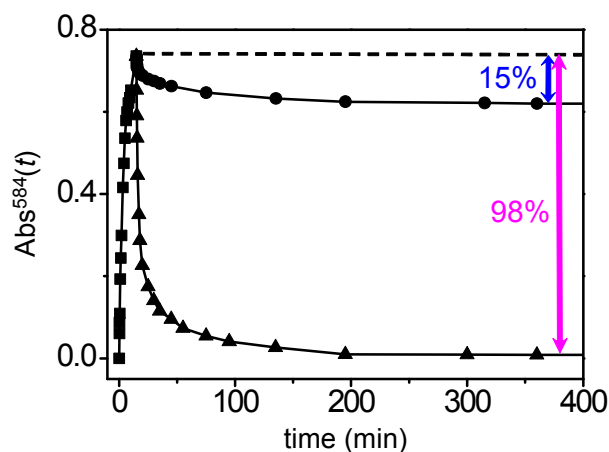


Figure SI19. Evolution of the maximum of the photogenerated absorption at $\lambda_{\max} = 584$ nm for $(\text{SP})_3\text{MnMo}_6\text{O}_{18}(\text{SN})_2$ during successive coloration/bleach cycles at room temperature. For one cycle, the sample is exposed to 365-nm UV irradiation for 1 min, and to yellow light for 15 min (the black lines display the mean values of the absorption in the coloured and bleached states).

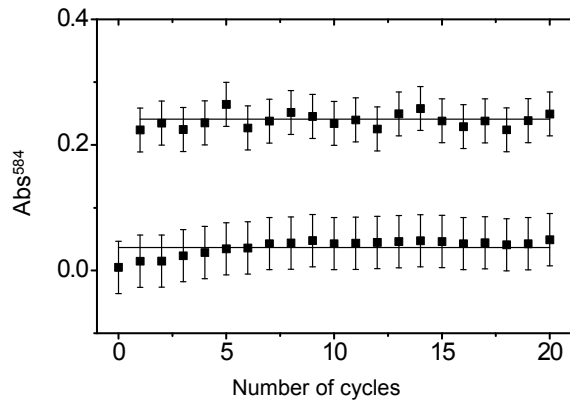


Figure SI20. $\text{Abs}^{600}(t)$ vs. luminous exposure plots for $\text{MnMo}_6\text{O}_{18}(\text{SN})_2$ at different light intensity at room temperature

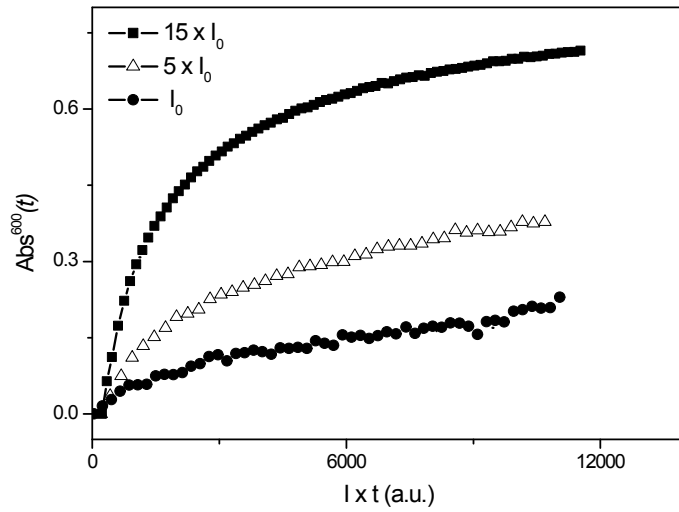
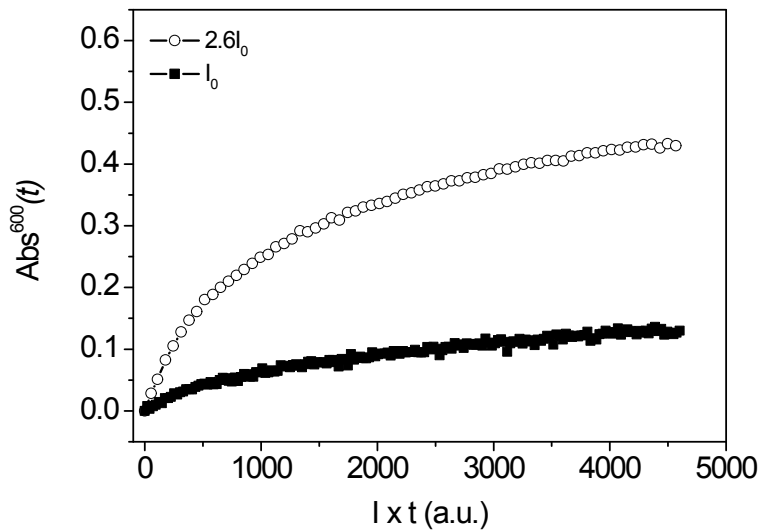


Figure SI21. $\text{Abs}^{600}(t)$ vs. luminous exposure plots for $\text{MnMo}_6\text{O}_{18}(\text{SP})_2$ at different light intensity at room temperature



NB: The value of $\text{Abs}^{600}(t)$ at saturation does not increase linearly with the light intensity for both samples. Several possible explanations can be suggested to understand the origin of these non-linear effects: (i) the role of the light absorption inside the sample and the dependence of the extinction coefficient on the light intensity; (ii) the presence of interactions between the molecules which hinder the photo-excitation process or (iii) the existence of a photo-heating effect for large intensity values which may produce important thermal gradients in the sample, resulting in a non-linear response of the absorption spectra with time

Figure SI22. Temporal evolutions of the reflectance signal at 600 nm for $\text{MnMo}_6\text{O}_{18}(\text{SN})_2$ at different temperatures. The stationary states reached after long time measurements depend non-linearly on temperature.

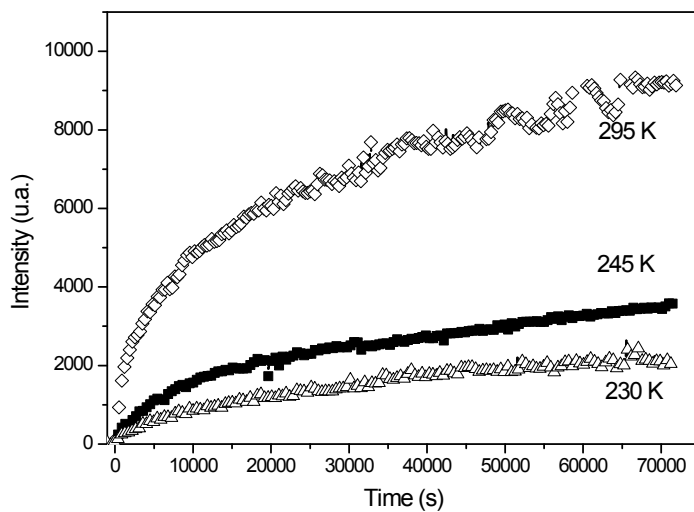


Table SI1. Crystallographic data for complex **MnMo₆O₁₈(SP)(SN)**

Chemical formula	C ₅₃ H ₅₄ Mn Mo ₆ N ₆ O ₃₀
M_r (g.mol ⁻¹)	1885.60
Cell setting, space group	Monoclinic, C2/c
Temperature (K)	199 (2)
a, b, c (Å)	34.953 (2), 23.0357 (14), 33.652 (2)
α, β, γ (°)	90.00, 104.105 (3), 90.00
V (Å ³)	26278 (3)
Z	8
D_x (Mg m ⁻³)	0.953
Radiation type	Mo K α
μ (mm ⁻¹)	0.693
Crystal form, colour	Parallelepiped, colorless
Crystal size (mm)	0.30 × 0.24 × 0.04
Diffractometer	Bruker APEX-II CCD
Data collection method	ϕ and ω scans
Absorption correction	Multi-scan (based on symmetry-related measurements)
T_{\min}	0.8191
T_{\max}	0.9728
No. of measured, independent and observed reflections	206961, 23097, 7323
Criterion for observed reflections	$I > 2\sigma(I)$
R_{int}	0.1674
θ_{\max} (°)	25.10
Refinement on	F^2
$R[F^2 > 2\sigma(F^2)], wR(F^2), S$	0.0857, 0.2228, 0.859
No. of relections	7323 reflections
No. of parameters	543
H-atom treatment	Constrained to parent site
Weighting scheme	Calculated $w = 1/[\sigma^2(F_o^2) + (0.1327P)^2 + 0.0000P]$ where $P = (F_o^2 + 2F_c^2)/3$
$(\Delta/\sigma)_{\max}$	0.127
$\Delta\rho_{\max}, \Delta\rho_{\min}$ (e Å ⁻³)	1.423, -0.842

Table SI2. Crystallographic data for complex **MnMo₆O₁₈(SN)₂**

Chemical formula	C ₅₆ H ₅₆ Mn Mo ₆ N ₆ O ₂₈
M_r (g.mol ⁻¹)	1891.65
Cell setting, space group	Monoclinic, C2/c
Temperature (K)	200 (2)
a, b, c (Å)	34.7751 (15), 23.3403 (10), 33.6814 (14)
α, β, γ (°)	90.00, 103.352 (2), 90.00
V (Å ³)	26599 (2)
Z	8
D_x (Mg m ⁻³)	0.945
Radiation type	Mo K α
μ (mm ⁻¹)	0.684
Crystal form, colour	Parallelepiped, colorless
Crystal size (mm)	0.25 × 0.20 × 0.08
Diffractometer	Bruker APEX-II CCD
Data collection method	ϕ and ω scans
Absorption correction	Multi-scan (based on symmetry-related measurements)
T_{\min}	0.8477
T_{\max}	0.9473
No. of measured, independent and observed reflections	270897, 23391, 14490
Criterion for observed reflections	$I > 2\sigma(I)$
R_{int}	0.0593
θ_{\max} (°)	25.09
Refinement on	F^2
$R[F^2 > 2\sigma(F^2)], wR(F^2), S$	0.0920, 0.2960, 1.087
No. of relections	14490 reflections
No. of parameters	812
H-atom treatment	Constrained to parent site
Weighting scheme	Calculated $w = 1/[\sigma^2(F_o^2) + (0.1315P)^2 + 373.8951P]$ where $P = (F_o^2 + 2F_c^2)/3$
$(\Delta/\sigma)_{\max}$	0.225
$\Delta\rho_{\max}, \Delta\rho_{\min}$ (e Å ⁻³)	0.834, -0.76

Table SI3. Characteristics of UV-visible absorption spectra of **SNTris**, **MnMo₆O₁₈(SN)₂** and **MnMo₆O₁₈(SP)(SN)** in DMF + 0.2M LiClO₄.

Compound	λ1/nm (ε/M ⁻¹ cm ⁻¹)	λ2/nm (ε/M ⁻¹ cm ⁻¹)	λ3/nm (ε/M ⁻¹ cm ⁻¹)
MnMo₆O₁₈(SP)(SN)	325 (16100)	353 (16140)	372 (12300)
MnMo₆O₁₈(SN)₂	325 (13700)	356 (10300)	372 (7700)
SNTris	325 (10000)	356 (7600)	372 (5800)

Table SI4. Photo-coloration kinetic parameters of **MnMo₆O₁₈(SP)(SN)**, **MnMo₆O₁₈(SN)₂**, **MnMo₆O₁₈(SP)₂**, **(SP)₃MnMo₆O₁₈(SN)₂**, **SNTris**, and **(SP)I**.

	MnMo₆O₁₈(SP)₂	MnMo₆O₁₈(SP)(SN)	MnMo₆O₁₈(SN)₂	SNTris	(SP)₃MnMo₆O₁₈(SN)₂	SP(I)
λ_{max}^a (nm)	570	570	620	620	584	584
A ₁ ^b	-0.590	-0.496	-0.459	-0.544	-0.038	-0.433
A ₂ ^b	-0.536	-0.377	-0.300	-0.276	-0.018	-0.415
k ^c ₁ × 10 ³ (s ⁻¹) ^c	15.1 ± 1.9	16.6 ± 1.4	13.0 ± 0.9	11.1 ± 0.7	1.6 ± 0.2	7.3 ± 0.0
k ^c ₂ × 10 ³ (s ⁻¹) ^c	4.3 ± 0.7	4.1 ± 0.5	2.5 ± 0.4	2.0 ± 0.5	10.4 ± 2.2	1.4 ± 0.5
R ^d	0.9993	0.9994	0.9993	0.9992	0.9965	0.9981
						0.9996

^aPhotoinduced absorption band wavelength. ^bThe Abs^{λmax}(t) vs t plots were fitted as Abs^{λmax}(t) = -A₁-A₂ + A₁exp(-k^c₁t) + A₂exp(-k^c₂t). ^cColoration rate constants. ^dRegression coefficient for the Abs^{λmax}(t) vs t plots

Table S15. Fading kinetic parameters of **MnMo₆O₁₈(SP)(SN)**, **MnMo₆O₁₈(SN)₂**, **MnMo₆O₁₈(SP)₂**, **(SP)₃MnMo₆O₁₈(SN)₂**, **SNTris**, and **(SP)I** exposed under yellow light irradiation.

	MnMo₆O₁₈(SP)₂	MnMo₆O₁₈(SP)(SN)	MnMo₆O₁₈(SN)₂	(SP)₃MnMo₆O₁₈(SN)₂
λ_{max} (nm)	570	570	620	584
A ₀	1.058	0.860	0.730	0.767
A ₁	0.525	0.609	0.455	0.405
A ₂	0.533	0.056	0.108	0.275
$k'_1 \times 10^3$ (s ⁻¹)	0.15 ± 0.01	0.2 ± 0.0	0.3 ± 0.0	0.7 ± 0.1
$k'_2 \times 10^3$ (s ⁻¹)	0.15 ± 0.01	26.1 ± 6.6	25.9 ± 4.6	36.8 ± 3.5
R ²		0.9986	0.9971	0.9970
				0.9965

Table S16. Thermal fading kinetic parameters of **MnMo₆O₁₈(SP)(SN)**, **MnMo₆O₁₈(SN)₂**, **MnMo₆O₁₈(SP)₂**, and **(SP)₃MnMo₆O₁₈(SN)₂** maintained in the dark.

	MnMo₆O₁₈(SP)₂	MnMo₆O₁₈(SP)(SN)	MnMo₆O₁₈(SN)₂	(SP)₃MnMo₆O₁₈(SN)₂
	MnMo₆O₁₈(SP)₂	MnMo₆O₁₈(SP)(SN)	MnMo₆O₁₈(SN)₂	(SP)₃MnMo₆O₁₈(SN)₂
λ_{max} (nm)	570	570	620	620
A ₀	1.059	0.863	0.732	0.764
A ₁	0.069	0.128	0.161	0.326
A ₂	0.017	0.044	0.069	0.234
$k'_1 \times 10^3$ (s ⁻¹)	0.08 ± 0.01	0.18 ± 0.0	0.27 ± 0.0	0.3 ± 0.0
$k'_2 \times 10^3$ (s ⁻¹)	5.9 ± 0.84	31.5 ± 3.3	32.4 ± 4.0	10.5 ± 1.2
R ²	0.9968	0.9976	0.99633	0.9962
				0.9952

Table SI7. Photo-coloration kinetics parameters for $\text{Abs}^{600}(t)$ vs. t plots of $\text{MnMo}_6\text{O}_{18}(\text{SN})_2$ for different temperatures.

	A_1	A_2	$k^c_1 (\text{s}^{-1})$	$k^c_2 (\text{s}^{-1})$
200K	-0.41(1)	-0.43(1)	0.0030(1)	0.00037(2)
150K	-0.13(1)	-0.37(0)	0.0025(2)	0.00026(1)
125K	-0.08(2)	-0.30(0)	0.0018(7)	0.00019(6)
87K	-0.063(10)	-0.32(3)	0.0014(2)	0.00012(3)

Table SI8. Photo-coloration kinetics parameters for $\text{Abs}^{600}(t)$ vs. t plots of $\text{MnMo}_6\text{O}_{18}(\text{SP})_2$ for different temperatures.

	A_1	A_2	$k^c_1(\text{s}^{-1})$	$k^c_2(\text{s}^{-1})$
200K	-0.76(2)	-0.41(1)	0.0058(2)	0.00063(4)
150K	-0.79(1)	-0.26(1)	0.0051(2)	0.00046(2)
94K	-0.53(1)	-0.41(1)	0.0037(3)	0.00044(2)

ⁱ P. van der Sluis, and A. L. Spek, *Acta Crystallogr., Sect. A.*, 1990, **46**, 194.